19th IAHR International Symposium on Ice
"Using New Technology to Understand Water-Ice Interaction"
Vancouver, British Columbia, Canada, July 6 to 11, 2008

Acoustic Detection and Study of Frazil Ice in a Freezing River during the 2004-2005 and 2005-2006 Winters

John R. Marko,
ASL Environmental Sciences Inc.
and
Martin Jasek
BC Hydro Ltd.

Results are reported from two annual measurement programs carried out on the Peace River which demonstrated near-realtime capabilities for detailed monitoring of frazil ice particles suspended in the water column using upward-looking acoustic profilers. Prior to local stabilization of the seasonal ice cover, frazil ice was fund to be present only during intervals of measurable supercooling when it was characterized by target strengths uniformly distributed through the middle and upper water column. Ice cover stabilization changed this situation, allowing detection of frazil-like targets at all times but with the upper water column now dominated by the presence of a layer of mobile ice particles associated with target strengths which increased sharply with height. Beneath the stable ice cover, target strength variations in the water column were found to be significantly correlated with both lower frequency variations in regional air temperature and with higher frequency changes in local water levels. Our observations were most consistent with both frazil generation in upstream open water areas and the existence of unknown mechanisms whereby local water level- and/or water speed-dependent processes control the vertical distributions of frazil in the water column beneath the stabilized downstream ice cover. The implications of these results for current models of freezing rivers and for the design of subsequent winter river monitoring and study programs will be discussed.

1. Introduction and Description of Measurements

Suspended individual or aggregated crystals of frazil ice in fresh water bodies often have significant impacts upon water supply, hydro electric, fisheries and other management activities. Effective detection and quantitative characterization of such ice can provide direct input to operational decision-making and for formulating numerical river ice and flow models (Shen, 2006) underlying modern flow management (Jasek, 2006). This note presents results from two recent winter deployments of acoustic profilers in the Peace River, Alberta, Canada which demonstrate near-realtime capabilities for quantitatively assessing suspended frazil content and its sensitivities to environmental factors. The utilized upward–looking sonar measurement technique extends an ice profiling technology originally developed (Melling et al., 1995) to obtain (Melling and Reidel, 1995, Marko, 2003) marine ice draft data from self-contained moored instruments. With a few notable exceptions, collected data have been specific to drifting surface ice. In one of the exceptions, "draft" data from the Bering Sea were used (Drucker et al., 2003) to deduce penetration depths of frazil ice entrained in Langmuir circulation plumes. More recently, Leonard et al. (2006) have used ADCP current profiler signal amplitude data to estimate "platelet" or frazil ice concentrations beneath Antarctic multi-year ice.

The results presented here were obtained in freshwater during B.C. Hydro's 2004-2005 and 2005-2006 winter Peace River monitoring programs utilizing SWIPS (Shallow Water Ice Profiler Sonar) instruments developed by ASL Environmental Sciences Inc. from the company's IPS4 Ice Profiler platform. Aside from changes in acoustic frequency, the principal distinction of the SWIPS was confinement of all active components, exclusive of the transmitting/receiving transducer and tilt, pressure and temperature sensors, to a sheltered shoreline enclosure. This change minimized risks of loss or damage of control and data storage components and facilitated access to data for opportunistic changing of measurement parameters. The wet instrument components were mounted on a heavy concrete block, deployed on the river bed and linked to the shore station by 150 m power and communication cables. Measurement parameters, such as the ping or acoustic pulsing rate (usually 1 Hz), the numbers of consecutive pings emitted in each sampling interval (burst) and the separations between sampling intervals, were remotely set based upon data periodically uploaded from the unit's 65 Mb flash memory. Data-taking alternated, at selectable intervals, between a conventional range-finding mode (whereby ranges to the river-air interface or to the ice undersurface were automatically estimated) and a, more data-intensive, true profiling mode which recorded acoustic return amplitudes from each, roughly, 2 cm deep horizontal slice of the insonified water column. This operational mode was essential for frazil ice detection.

Two different SWIPS instruments were deployed: a low frequency 235 kHz SWIPS1 unit, utilized in both annual programs; and a 545 kHz, high frequency, SWIPS2 unit during only the 2005-2006 study. The general location of the SWIPS1 unit was similar in its two deployments although the 2005-2006 site was in shallower water (3.4 m vs. 6m). The original SWIPS2 site was in 5 m of water about 10 to 20 m offshore of the SWIPS1. Measurements of snow, thermal and slush ice thicknesses were carried out from the stabilized ice cover on three dates in the January-March, 2005 period, accompanied by field and laboratory acoustic transmission and scattering studies. 2005-2006 field efforts were limited to estimating river drift speeds after ice

clearance. Instruments were in place from early November through to May and meteorological data were routinely collected at local and upstream Environment Canada gauging sites.

2. Frazil-Related Results from 2004-2005 Program

Although the 2004-2005 SWIPS1 deployment was directed at documenting surface ice draft, data gathered prior to stabilization (immobilization) of the ice cover in early January, 2005 also showed evidence of occasional, weak, water column targets suggestive of suspended frazil ice presence. In each case, targets coincided with observations of the supercooled (temperatures < 0ºC) river water required for frazil formation. Initially, these targets appeared to disappear from the water column after stabilization, presumably due to absence of supercooling beneath a stable, insulating, ice cover. Later, however, similar but more persistent weak returns were detected down to depths extending, roughly, 1 m below the ice cover. Such returns were mostly confined to the period February 24-March 16 and are apparent in the hourly-averaged return strength profiles of Figure 1. A video survey on March 2 showed the presence of large concentrations of drifting frazil flakes at the depths associated with the anomalous returns. Comparable concentrations of frazil flakes were also observed on February 3 which were, however, not readily detectable in the SWIPS record. The stabilized ice cover, itself, showed characteristically weaker returns from its lower reaches which were comprised of porous slush ice. This lower ice layer, according to both SWIPS and field measurements, grew thinner over time, indicative of progressive dissipation and partial conversion into the harder "thermal" ice associated with the upper portions of the ice cover. Ranges corresponding to the modeled and measured positions of the bottom of the thermal ice are included in Figure 1 for reference purposes, although comparisons of actual and acoustically-estimated ranges to points internal to the ice cover points are problematic due to the uncertain composition dependences of the anomalously low sound speeds (relative to water values) detected in the lower ice cover (Jasek et al., 2005).

3. Results from 2005-2006 Program

Evidence of frazil–detection during the 2004-2005 program motivated inclusion of a 546 kHz SWIPS2 unit in the 2005-2006 study program. The higher frequency of this unit was intended to increase detection sensitivity based upon expectations that the scattering cross-sections of frazil particles with radii, $a < \lambda/2\pi$, where λ is the acoustic wavelength, followed a Rayleigh Law proportionality to the fourth power of acoustic frequency. After corrections for different system gains, SWIPS2 return signal strengths were anticipated to exceed SWIPS1 returns from common targets by 33.6 dB. The resulting sensitivity increases are evident in comparisons (Figures 2a, b) of, roughly, 48 hours of coincident SWIPS1 and SWIPS2 profile data presented as target strengths vs. range for successive returns from bursts of 120 1 s-separated pings. The bursts were emitted at half-hour intervals during a January 11-13, 2006 time interval associated with cold air temperatures and supercooling. Two separate intervals of frazil detection were apparent characterized by essentially range-independent average target strengths for ranges (heights) > 1m above the bottom-mounted transducer. Detection duration was relatively brief, about 3 hours, in the first interval (initiated around 08:00, January 12) but a second, more intense, event followed at about 17:00 on the same day and persisted almost to the end of the depicted period. Averaged over a 2.5 hour period, the strongest of the SWIPS1 water column returns (Figure 2a) in the latter period were comparable to the maximal returns observed with the same instrument

during the 2004-2005 program. This level was approximately 30.7 dB +/- 3 dB below corresponding SWIPS2 return levels, in accord with anticipated sensitivity differences. This agreement validated the Rayleigh scattering assumption and its underlying target size restrictions, suggesting that detected particle diameters were on the order of and smaller than about 0.8 mm.

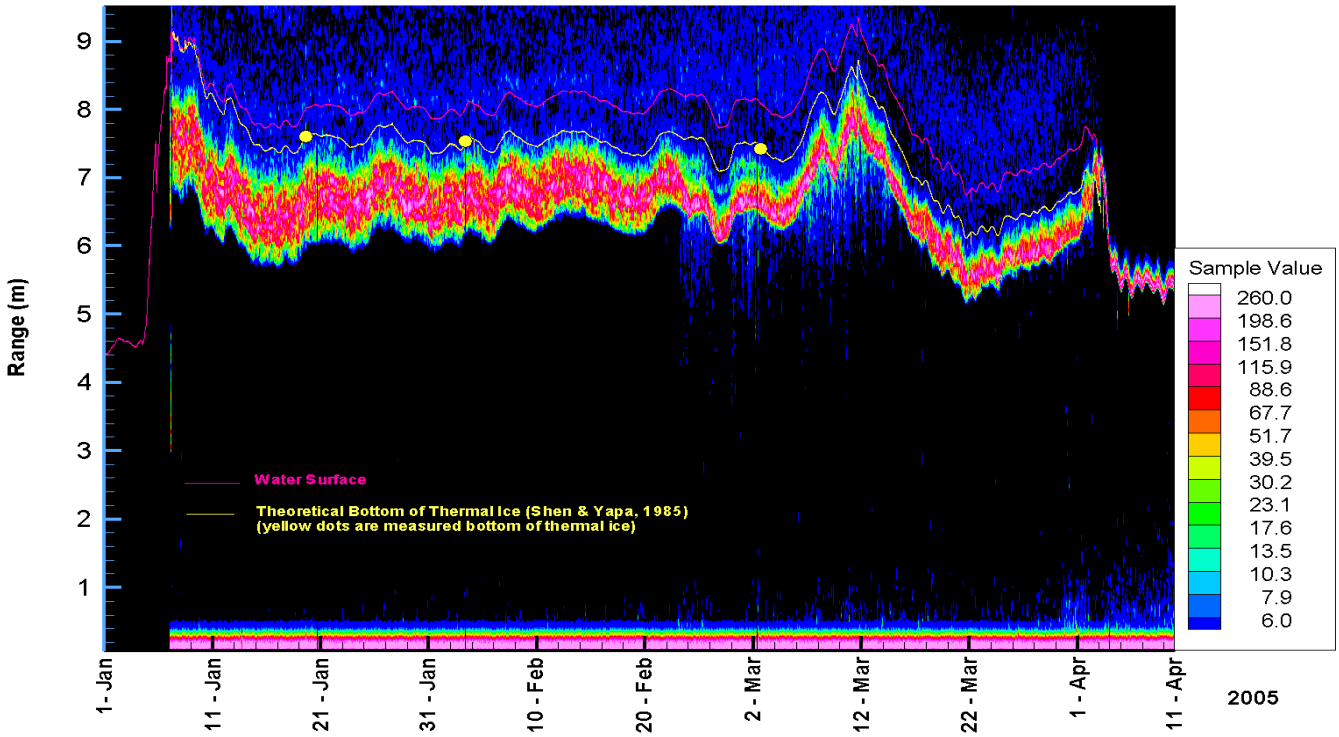

Figure 1. Plots of January-April, 2005 hourly averaged SWIPS1 return signal amplitudes in counts, local water levels and measured and modeled positions of the thermal ice undersurface.

Shortly after these observations were made, accumulations of anchor ice on both instruments temporarily blocked the acoustic beams, interrupting data collection. Even worse, buoyancy contributions from ice affixed to the concrete instrument platforms and cables produced uncontrolled changes in instrument positions and orientations. The SWIPS1 platform was overturned, ending its meaningful data collection. The SWIPS2 was fortuitously stabilized in slightly deeper water (by 1.5 m) in late January with its acoustic beam tilted 66º off vertical. A subsequent warming period initiated anchor ice clearance and resumption of SWIPS2 data gathering, albeit with a tilted acoustic beam. Although complicating interpretation of returns from surface ice, beam tilting did not preclude frazil ice monitoring since the isotropic scattering expected from particulate targets still allowed extraction of acoustic return strengths as a function of height in the water column, using the cosine of the tilt angle for range to height conversion. The validity of this approach was verified by noting the close similarity of profiles in equivalently intense supercooling intervals as detected, respectively, prior to and after tilting of the SWIPS2 beam (see the Jan. 13 and Feb. 25 profiles in Figure 3a).

Between February 15 and the February 28 date of local ice cover stabilization, the tilted SWIPS2 beam also detected distinctively stronger returns from moving surface floes with typical maximum drafts on the order of 0.75 m. Returns from water column frazil in this period were

found to be either of low or negligible strength approximately 50% of the time, based upon the representative return levels displayed in Figure 3a,. Figure 3a also includes May data, acquired to illustrate ice-free background return levels. The general form of the pre-stabilization frazil profile included intense near-bottom returns (believed to arise from suspended sediments) which fell off sharply with height above the transducer. The steep slopes of the curves shallowed significantly approximately 0.6 m above the transducer, producing characteristically depth-independent returns from heights between 2m and the bottom of the ice cover.

Local stabilization of a seasonal ice cover typically moves up-river as drifting floes and underlying frazil slush eventually slow into immobility. The "ice front" marking the boundary between the stabilized (downstream) and mobile (upstream) portions of the ice cover progressively advances upstream over the course of seasonal development. The sharply higher water levels accompanying local stabilization are more or less sustained through to breakup and maintain throughput of water from unstabilized upstream areas. The 2004-5 data showed the stabilized ice cover to be a mix of the hard "thermal" constituent of drifting floe ice and an underlying, initially thicker, layer of slushy, consolidating frazil ice with the lower boundary of the hard ice progressively advancing over time into the dissipating and eventually (shortly before breakup) disappearing slush layer (see Jasek et al., 2005). Local frazil generation should be largely absent beneath a stabilized local ice cover and additional upstream advances of the ice front might be expected to progressively diminish the local presence of frazil drifting downstream from increasingly more distant open water production areas. Such conditions beneath a stable ice cover are consistent with the bulk of the 2004-2005 low frequency (SWIPS1) data of Figure 1 apart from the anomalous February- March period and video results (Jasek et al., 2005) which were suggestive of a layer of ice particles extending down to depths at least 1m below the ice cover, possibly arising from erosion at the adjacent ice undersurface.

The 2005-2006 results, acquired at the higher SWIPS2 acoustic frequency, on the other hand, were characterized by the continuous presence of significant frazil returns with strengths often exceeding those of the strongest pre-stabilization returns, particularly at heights beyond pre-stabilization water levels. This situation is illustrated by the six-hour averaged profiles of Figure 3b plotted for stabilized ice cover periods associated with, respectively, near minimal and near maximal acoustic return strengths. The two other curves in the Figure represent data acquired at times prior to ice formation and following break-up and clearance, respectively. The latter, baseline, responses show zones of strong close-in returns with dimensions (1m) essentially identical to those observed beneath the mobile ice cover (Figure 3a). The smaller dimensions of such zones in the stabilized ice cover profiles, indicative of compression of the turbulent bottom boundary layer, are a likely consequence of the presence of the additional boundary layer at the stabilized ice cover. The sharp rises at the upper ends of the stabilized ice cover curves encompassed water column heights, roughly, up to 1m below contemporary river water levels. In the absence of on-ice measurement data, insights on the latter, high-lying, strong scattering regime responsible for these rises were drawn from time series profile depictions such as that of Figure 4 corresponding to returns from two bursts of 60 1s-separated pings emitted 30 minutes apart in a March 17 time interval associated with a local minimum in target strength. The key features of the depiction are the distinctive slopes of returns from both strong targets at heights $\geq$ 5.5 m as well as from much rarer and weaker targets deeper in the water column. Such slopes arise from the fact that targets which retain physical coherence in a tilted acoustic beam over the

1 s pinging intervals are detected at progressively larger ranges as they move through the beam footprint. These results, thus, suggest that acoustic returns from vertical heights ≤ about 7.3 m above the SWIPS transducer were often associated with extended targets moving with velocities comparable to the projected horizontal water velocity component. (Comparisons with independent river speed estimates indicated that the tilted beam azimuth deviated by approximately 41º from the local flow direction.) Returns from still higher levels in the water column were excluded from the Figure to avoid contributions from more slowly moving, non-particulate, portions of the stable ice cover (Jasek et al., 2005).

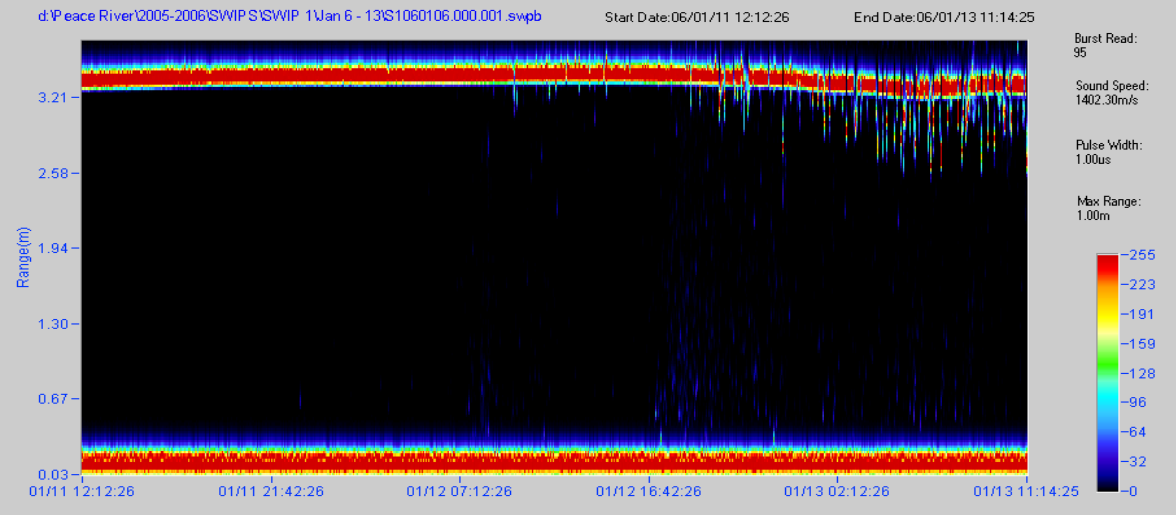

Figure 2a. 235 KHz unit data- Initial low frequency results show weak returns from the water column (depths less than 2.94m) appearing primarily after 07:00 1/12.

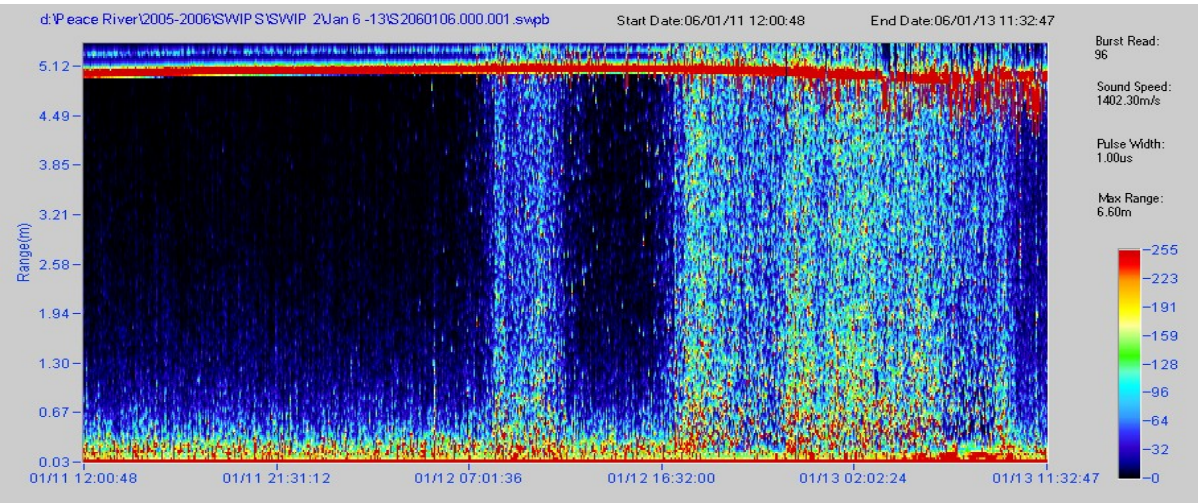

Figure 2b. 546 kHz unit data- High frequency results show full range of return variability in same intervals associated with frazil ice presence (depths less than 4.8 m).

Unfortunately, use of profile data for extracting the detailed composition of water column ice particle content remains problematic in the absence of multi-frequency data which could separately estimate particle number density and size distribution parameters. Thus, the observed sharp rise in target strength at heights greater than 5.5m could be a consequence of increases in

either or both particle numbers and sizes. An intriguing possibility in this respect arises from the well known (Martin, 1981) tendency of frazil particles to sinter or bond together: increasing buoyancy to drag force ratios and, consequently, relative probabilities for occupying upper portions of the water column. This possibility, alone, because of the sixth power particle diameter dependence of Rayleigh scattering cross-sections, could account for rising target strengths at the upper ends of the stabilized ice cover curves (Figure 3b). Clarifications of this and other frazil composition issues clearly require expanded measurement programs. Guidance for such programs is sought below by using the 2005-2006 data to explore empirical relationships between frazil-related target strengths and relevant environmental factors.

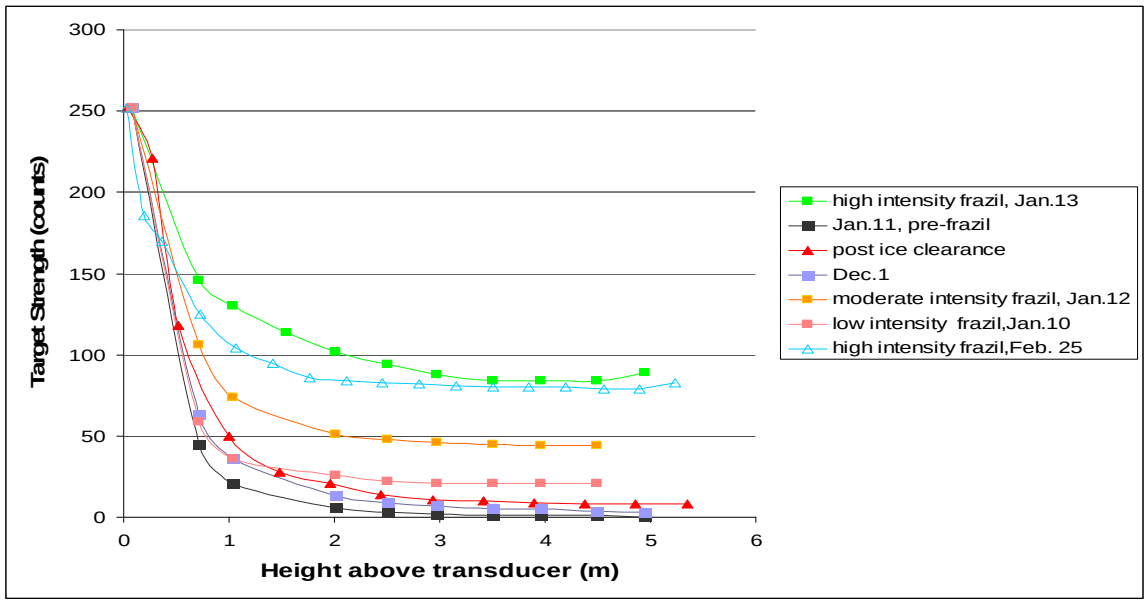

Figure 3a. Six-hour averaged target strength (counts) vs, height (m) above the transducer at indicated times. Square- (triangle-) denoted data were obtained with vertical (tilted) beams.

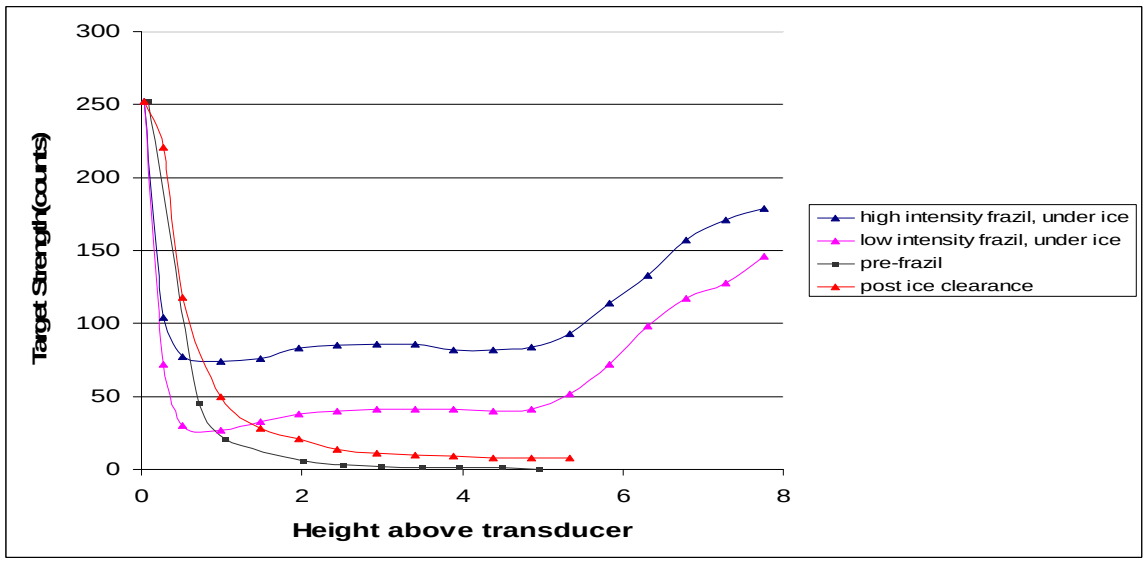

Figure 3b. Six-hour averaged SWIPS2 target strength vs. height above the transducer under the indicated conditions. Again, squares (triangles) denote vertical (tilted) beam data.

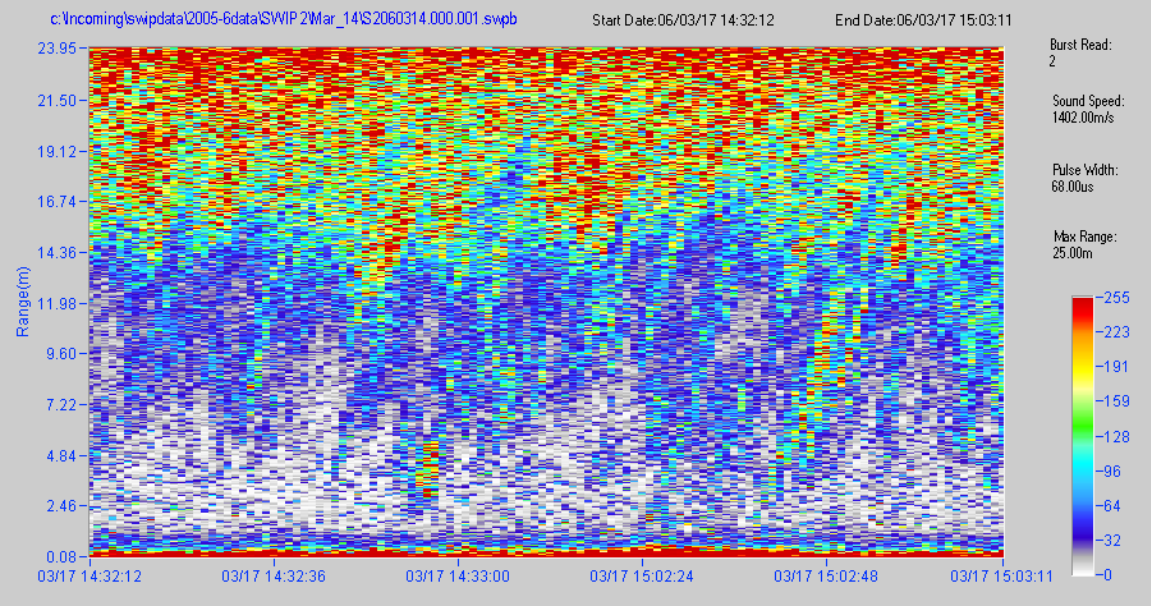

Figure 4. High temporal resolution SWIPS2 returns from 2 bursts of 60 pings emitted at 1 Hz at opposite ends of a 30 minute March 17, 2006 time interval.

4. Frazil Target Strength beneath a Stabilized Ice Cover: Environmental Dependences

The anticipated absence of frazil ice growth beneath a stable ice cover is consistent with the corresponding cessation of anchor ice-interruptions of SWIPS2 measurements. The measurement continuity was notable relative to earlier, pre-stabilization, behavior and persisted despite the fact that frazil-related target strengths increased to levels comparable to and, often, larger than those of the most intense pre-stabilization frazil episodes. Consequently, key environmental determinants of suspended frazil variability under stabilized ice covers might be expected to act through either generation and export of frazil from adjacent upstream regions and/or through controlling ice cover deterioration rates. The latter possibility could, in principle, produce variations in water column ice content without generating "new" frazil. The obvious candidate parameters for such influences are local and upstream air and water temperatures, river flow velocities and the positions of the ice front. Near-bottom water temperatures measured at the SWIPS1 instrument showed no evidence of either supercooling or warming except at the tail end of the ice-covered period and, hence, were unlikely to be directly linked to the observed variability. Air temperature held greater promise as a forcing factor and values measured at hourly intervals 7 km downstream from the SWIPS site were found to be representative both of that site and areas near and upstream of the documented ice front positions (Figure 5). Water speed estimates were available only indirectly from models and empirical relationships to water levels deduced from SWIPS1 hydrostatic pressure data: making such levels a parameter of potential importance both on its own and as a river speed proxy. Environmental parameter comparisons were made with measures of acoustic target strength expressed in terms of averages over heights in the water column corresponding to mid- and upper-water column layers as defined by, respectively, heights between 2 to 5 m and 5 to 7.3 m. These choices reflect the obvious changes in target strength regime apparent in the under-ice data of Figure 3b.

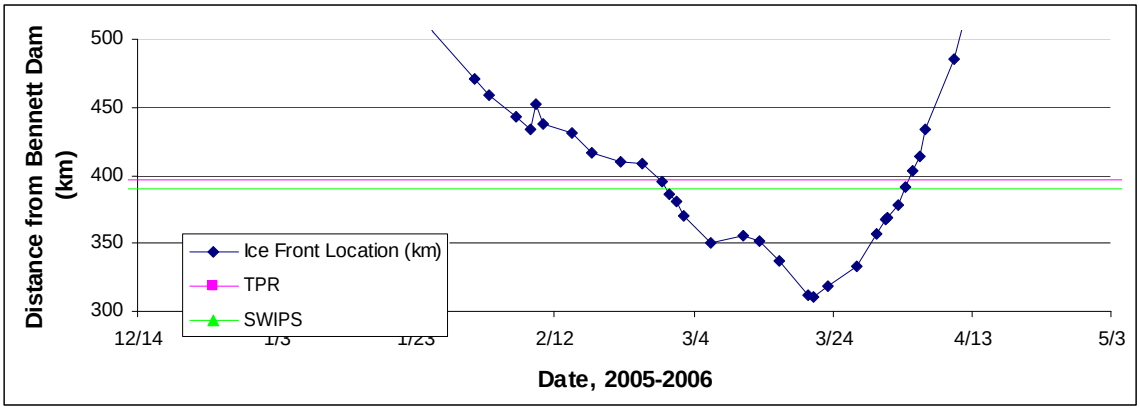

Figure 5. Locations (in km downstream of a dam reference position) of the 2005-2006 ice fronts and the SWIPS and air temperature measurement sites.

Time series of target strengths in each layer were averaged over height and each half-hourly burst interval and passed through a 4-hour running average filter to allow comparisons with both each other and with corresponding air temperatures and water levels. As expected from Figure 3b, the target strengths in the two layers followed each other closely, corresponding to r = 0.71 over the full record and r = 0.84 when a 40 hour March 15-16 period of obviously disparate behavior was excluded. Maximum target strength magnitudes bracketed the 103 count average values associated with the most intense pre-stabilization frazil episode depicted in Figure 2b. Comparisons with air temperature and water level data also showed correlations: first, in terms of similarities between the broad peaks in the target strength time series and in corresponding temperature and water level minima; and, then, in higher frequency components of variability.

Explorations of these correspondences were complicated by correlations between the environmental parameters themselves which arose from both the direct influence of the atmosphere on river conditions and from adjustments in the managed river flow in response to weather-related power consumption needs. Flow variations were also connected to ice front position movements which either increased or decreased local flow when, alternatively, receding downstream or advancing upstream of the monitoring site. Our analyses applied additional (to the 4-hour filter) 24 hour running average low pass filtering to the hourly air temperature and half hourly water level and target strength time series, providing measures of variability on timescales longer than the, roughly, diurnal periodicities apparent in most of the data. Corresponding plots (Figure 6) show that a broad mid-March drop in air temperatures preceded similar decreases in target strength and rises in water levels. Over the full record, water levels lagged air temperature by about 55 hours with a correlation of r = 0.6. Air temperature/target strength correlations were r = -0.64 and -0.78 for the mid- and upper-water layers, respectively, with corresponding optimal lags of 0 and 75 hours. Excluding data from the period prior to March 9, associated with anomalous positive correlations, produced even stronger air temperature-target strength correlations (r values of -0.77 and -0.86 for the mid- and upper-water layers, respectively). Given the limited number of degrees of freedom associated with these data, the statistical significances of these comparisons are low but, particularly after the immediate post-stabilization period, are suggestive of physically reasonable negative correlations between target strengths and slow changes in regional air temperatures occurring 0 to 3 days earlier. Target strength correlations with water levels were also negative and similar in

magnitude and lag times but were of opposite sign (changes in water level lagging those in target strength). Indirect evidence, presented below, suggests that the latter results reflect water level linkages to the low frequency air temperature variations which drive similar temporal scale changes in water column target strength.

High frequency components of variability, as defined by the differences between singly (4-hour) filtered and doubly (4- and 24-hour) filtered time series data, showed much less ambiguous linkages of the middle and upper layer target strengths to both each other and to similar temporal scale water level variations. Such linkages are apparent in the difference time series plotted in Figure 7 for the water level- and mid- and upper-water layer-target strength parameters. Corresponding air temperature results, not included in the Figure for clarity purposes, also showed variations on similar time scales which were, however, devoid of a consistent relationship to the other plotted parameters. The plots show both the close tracking of the average target strengths in the adjacent water layers as well as the occurrence of short intervals when such tracking was absent. Prominent divergences in the behavior of the two layers were apparent on March 6 and 25 as well as in the March 15-16 interval cited above. As well, the high frequency target strength variations in both layers can be seen to have been closely coincident with corresponding components of water level change except, again, in a small number of short time intervals. Overall, rises and falls in target strength accompanied water level changes of the same sign with negligible time lags. It is notable that the positive signs of these correlations were opposed to those deduced above from our low frequency target strength/water level comparisons, supporting the conclusion that the latter correlations arose from low frequency linkages of both target strength and water level to air temperature. Over the full record, high frequency target strength/water level correlations of $r = 0.60$ and 0.50 relative to water levels were obtained for the mid-and upper water column layers, respectively. Still larger correlations, $r = 0.74$ and 0.67, were associated with these same pairings of parameters based upon data recorded after 13:00, March 17. These results reflect the general impression given by Figures 6 and 7 that the effects of water level changes were most apparent in the mid-water layer, possibly because of the greater direct linkages between upper layer target strength and air temperature.

Explanations of these results in terms of extraneous effects, such as physical oscillations of the tilted acoustic beam or flow-induced changes in frazil particle orientation were inconsistent with, respectively, tilt sensor data and the magnitude of the river speed changes. Moreover, empirical correlations with high frequency water level changes were found to be absent in data gathered with both tilted and untilted beams during period of frazil formation prior to stabilization. Since data from these periods were acquired upstream of contemporary ice fronts, this absence strongly suggests the high frequency target strength variations later observed under the stable ice cover were not consequences of frazil growth processes occurring in mobile ice and open water upstream of the SWIPS2 site. Consequently, the empirical linkages between water levels and target strengths suggested by the data in Figure 7 were unlikely to have been imposed upstream of the ice fronts but were of more local origin. On the other hand, the negative, probably time-lagged, target strength correlations with low frequency air temperature variations do suggest that more gradual changes in detected target strengths did arise from frazil production variations in areas upstream of the ice front. In this picture, physical mechanisms are required which allow high frequency variations in water level or speed to impose similar temporal scale changes upon frazil concentrations originally produced upstream of contemporary or recent ice fronts.

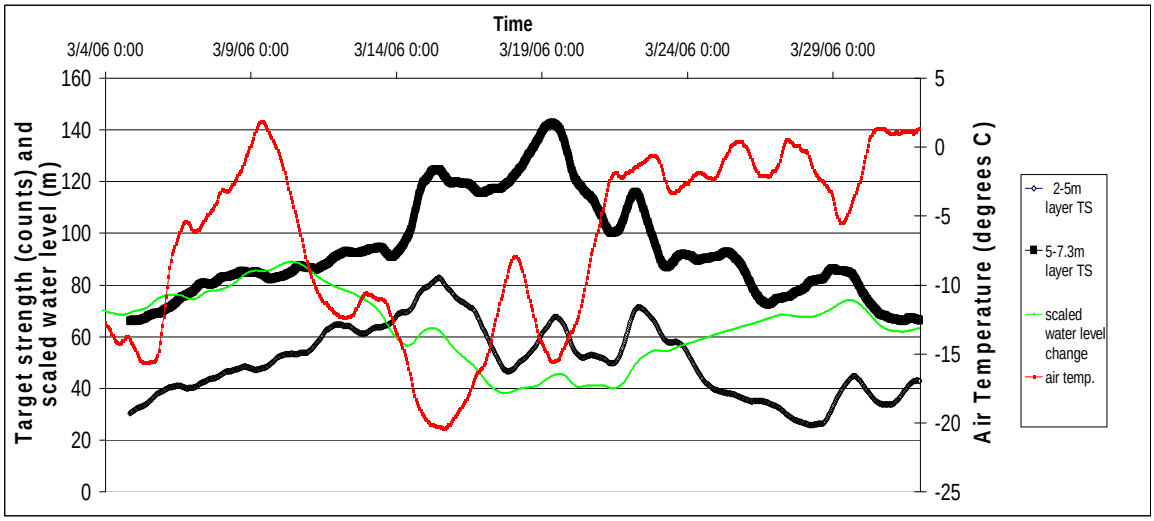

Figure 6. Time series plots of low frequency variability components in local water level, air temperature and mid- and upper-water column averaged target strengths. The water level changes were scaled as 70 × the difference between the measured water levels and 5.4m.

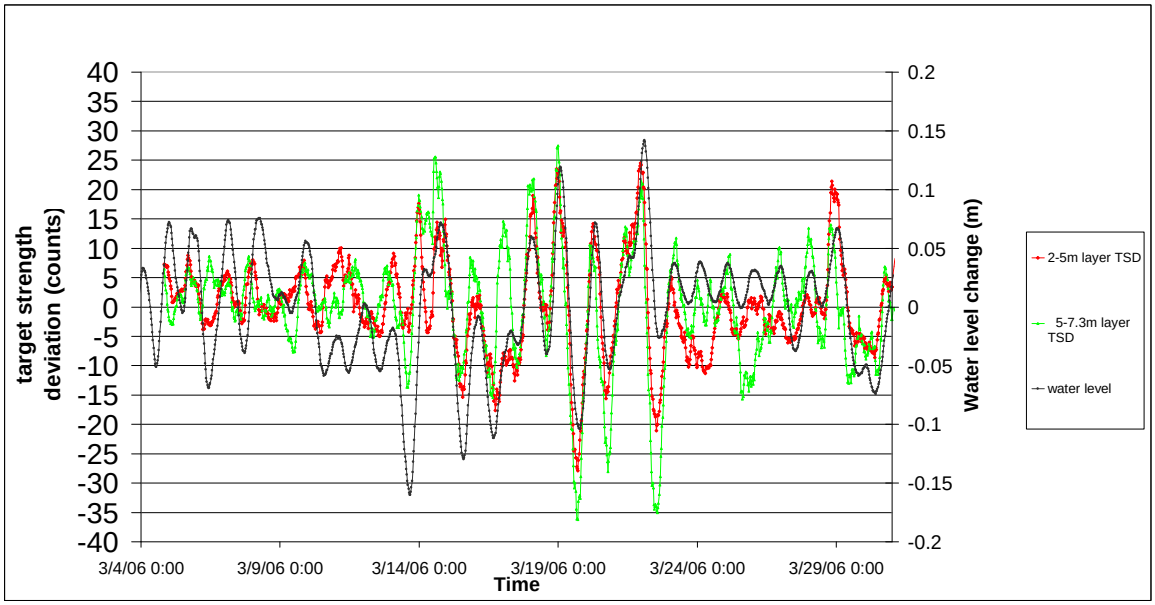

Figure 7. Time series plots of high frequency components of variability in local water level and mid- and upper-water column average target strengths.

Local processes can be visualized in which water level/speed variations either alter the contents of local deposits or, even, sources of frazil ice and/or control transport of upstream-generated frazil to these features and/or to the local water column. The observed negative correlations with air temperature changes appear to favor such mechanisms over ablation-based mechanisms for introducing ice particles into the water column. The observed sensitivities of target strength to height in the upper water column and to small changes in water level and/or flow speed may be indicative of the delicate balancing of frazil concentrations close to the ice cover against

dispersal deeper into the water column bulk. Slow movements detected on long (many hour) time scales at the nominal ice undersurface (Jasek et al., 2005) and the slanting profiles of Figure 4 suggest that ice targets near this interface move with speeds comparable to those of the river. Detailed documentation of this boundary regime and quantitative data on frazil particle size and number distributions as functions of height in the water column, river bathymetry and ice front positions are critical to understanding frazil ice variability beneath ice covers.

5. Summary and Conclusions

Field tests have demonstrated the capabilities of a higher frequency SWIPS profiler in monitoring frazil ice in freezing rivers. These tests have shown that, prior to local seasonal ice cover stabilization, frazil presence was confined to time intervals associated with measurable supercooling. In the absence of applied electrical heating, such intervals were plagued by anchor ice accumulations which, usually temporarily, interrupted monitoring. Target strengths at water column levels more than 2 m off the bottom varied negligibly with height. The presence of frazil ice targets was continuous beneath a stabilized ice cover in spite of the absence of supercooling and anchor ice formation. Target strength profiles under these conditions were readily distinguishable from their pre-stabilization counterparts, featuring a shallower zone of sediment-related near-bottom returns and a high-lying strong scattering layer which, presumably, included mobile ice particles at heights extending almost up to the nominal ice cover undersurface. Depth-averaged target strengths in the mid- and upper-water layers rose and fell in close concert and, at long temporal variability scales, showed lagged negative correlations with air temperature Strongest correspondences were noted between higher frequency variations in target strengths and water-level and/or -speed . Corresponding target strength fluctuations, sometimes equivalent to as much as 50% of mean strength values were well in excess of the accompanying percentage changes in water level or speed parameters. Such linkages were exclusive to the ice covered period, suggestive of origins in processes taking place in or beneath the stabilized ice cover. The observed behaviours appear to be directly relevant to monitoring and modeling ice growth and transport in freezing rivers and, hence, to power generation and flood control issues. Immediate future research needs include: multiple frequency measurements and calibrations to better characterize frazil properties as well as additional field and acoustic studies of the ice cover undersurface and the immediately adjacent water layer where water level and/or speed changes appear to affect water column frazil content.

Acknowledgments

Matt Stone, Jan Buermans, Vincent Lee, David Fissel of ASL Environmental Sciences; Kerry Paslawski of Timberoot Environmental; and Willi Granson, Alberta Environment all contributed to this work which was funded by BC Hydro, Alberta Environment and ASL.

References

Drucker, R., S. Martin, and R. Moritz, 2003. Observations of ice thickness and frazil ice in the St. Lawrence Island polynya from satellite imagery, upward looking sonar, and salinity/temperature moorings, J. Geophys. Res., 108 (C5),3149, doi:10.1029/2001JC001213.

Jasek, M., J.R. Marko, 2005. Instrument for detecting freeze-up, mid-winter and break-up processes in rivers. In Proceedings of 13th Workshop on Hydraulic of Ice-Covered Rivers (sponsored by CGU HS Committee on River Ice Processes and the Environment), Hanover, NH. 34p.

Jasek, M., 2006. Thermal ice growth model for managing hydropower production and reducing ice jamming on the Peace River. Proc. 18th IAHR International Symposium on Ice, Sapporo, Japan, Vol.1,107-116.

Leonard, G. H., C. R. Purdie, P. J. Langhorne, T. G. Haskell, M. J. M. Williams, and R. D. Frew, Observations of platelet ice growth and oceanographic conditions during the winter of 2003 in McMurdo Sound, Antarctica, J. Geophys. Res., 111, C04012, doi:10.1029/2005JC002952 , 2006.

Marko, J.R., 2003. Observations and analyses of an intense waves-in-ice event in the Sea of Okhotsk, J. Geophys. Res., 108 (C9), 3296, doi:10.1029/2001JC001214, 2003.

Martin, S., 1981. Frazil Ice in Rivers and Oceans Ann. Rev of Fluid Mechanics,13**,** 379-393, doi:10.1146/annurev.fl.13.010181.002115.

Melling,H., P.H. Johnson and D.A. Reidel , 1995.Measurement of the Draft and Topography of Sea Ice by Moored Subsea Sonar, J. Atmos. Oceanic Technol.13,.589-602.

Melling,H., and D.A. Reidel, 1996. Development of seasonal pack ice in the Beaufort Sea during the winter of 1991-1992: a view from below. J. Geophys Res. 101, 11975-11992.

Shen, H.T., 2006. A trip through the life of river ice-research: progress and needs. Proc. 18th IAHR International Symposium on Ic*e*, Sapporo, Japan, 9 p.